d.lp.

Closed-loop Control of Functional Neuromuscular Stimulation

NIH Neuroprosthesis Program Contract Number N01-NS-6-2338
Quarterly Progress Report #1
February 1, 1996 to April 30, 1996

Investigators:
Patrick E. Crago, Ph.D.
Clayton Van Doren, Ph.D.
Warren M. Grill, Ph.D.
Michael W. Keith, M.D.
Kevin Kilgore, Ph.D.
Joseph Mansour, Ph.D.
P. Hunter Peckham, Ph.D.
David Wilson, Ph.D.

Departments of
Biomedical Engineering,
Mechanical and Aerospace Engineering,
and Orthopaedics
Case Western Reserve University
and MetroHealth Medical Center

6/11/96 AAM

Table of Contents

1. SYNTHESIS OF UPPER EXTREMITY FUNCTION

The overall goals of this project are (1) to measure the biomechanical properties of the neuroprosthesis user's upper extremity and incorporate those measurements into a complete model with robust predictive capability, and (2) to use the predictions of the model to improve the grasp output of the hand neuroprosthesis for individual users.

1. a. BIOMECHANICAL MODELING: PARAMETERIZATION AND VALIDATION

Purpose

In this section of the contract, we will develop methods for obtaining biomechanical data from individual persons. Individualized data will form the basis for model-assisted implementation of upper extremity FNS. Using individualized biomechanical models, specific treatment procedures will be evaluated for individuals The person-specific parameters of interest are tendon moment arms and lines of action, passive moments, and maximum active joint moments. Passive moments will be decomposed into components arising from stiffness inherent to a joint and from passive stretching of muscle-tendon units that cross one or more joints.

Report of progress

1. a. i. MOMENT ARMS VIA MAGNETIC RESONANCE IMAGING

Abstract

A program is created to perform accurate tendon tracking in high resolution 3D MRI images. Image data are being acquired on an MRI system with unique capabilities for biomechanical imaging. We are optimizing the imaging methodology for accurate measurements. In the next quarter, we will be testing this method and creating other methods for measurement of tendon moment arm.

Progress Report

We are following the plan in the proposal. We will use 3D MRI to measure tendon moment arm. Our initial goal is to determine an accurate, practical method. Because of the difficulty with analyzing the wrist joint which is probably not well characterized as a hinge, we are first focusing on a simpler joint, the MCP joint of the index finger. As described in the proposal, we will examine at least 3 methods for analyzing tendon moment arm. They are: tendon excursion, 3D geometric, and 2D geometric. We are first focusing on the tendon excursion method.

Several steps are implemented in order to readily visualize the tendons in the index finger using MRI. First, we use a Siemens open magnet MRI system to acquire images. Unlike a conventional MRI system, this allows the subject to sit in a chair with his (her) arm resting on an imaging platform. On a conventional MRI system, the subject was forced to lie on his (her) stomach with arm extended overhead into the hand/wrist holder. The current situation is much more practical. To improve image quality, we now use a wrist coil. We spent several sessions optimizing imaging parameters to get optimal tendon and bone contrast. Currently, we think that there is some image degradation due to motion. Hence, we are creating a new wrist/hand holder. One feature is that it must allow the wrist coil to be placed near the anatomy to be imaged.

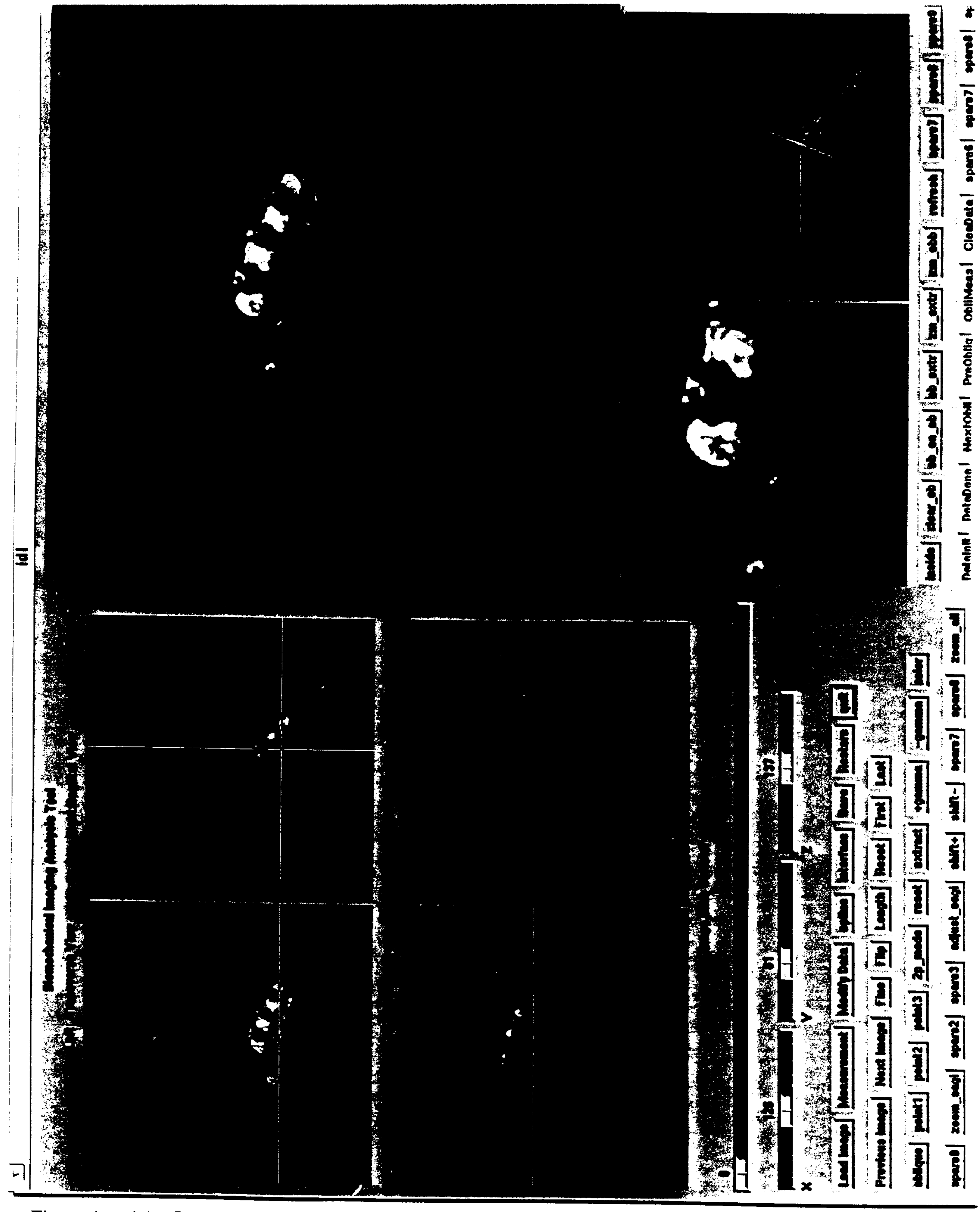

Figure 1. a. i.1. Interface of tendon tracking program.

We have created software for making accurate tendon excursion measurements and an example output is shown in Figure 1. a. i.1. In Figure 1. a. i.1 (left) there are 4 panels. In 3 of the panels, we demonstrate reformatting of the 3D image data sets into perpendicular planes aligned with the imaging system coordinates (x,y,z). The white overlay lines identify the cursor position in 3D space. This 3D cursor is used to mark the tendon. We recently added reformatting along an arbitrary surface. This allows one to place a reformatting surface along the length of bent fingers. This feature is illustrated in Figure 1. a. i.1 (bottom-right) where the two adjoining, long white lines indicate the reformatting surface. The small perpendicular line indicates a perpendicular surface which is displayed on the top-right. The remaining panel of the 3 on the right is a zoomed image. This reformatting operation improves visualization, and it enables us to more easily follow the tendon.

Using this interface, an operator manually traces a tendon along its length by marking the center of the tendon in zoomed images. When one places a mark in a transverse slice, the point is echoed in the two perpendicular views. These marks define a point in x,y,z space. We plan, but have not yet implemented, a method for center of mass calculation of the tendon center. After the operator traverses the tendon, a set of x,y,z points is obtained. A 3D spline is created to represent the tendon. Lengths are measured from the spline. We use bony landmarks in the image in order to look for length changes between the marks. Lengths are measured as a function of joint angle. Tendon moment arm is obtained from the derivative of excursion as a function of joint angle.

We validated the tendon length measurement technique by imaging a physical phantom consisting of curved Teflon rods. Measurements from the program closely match the actual size of the rods. We plan to redo this experiment with images having improved image quality.

We have not yet made a complete set of tendon measurements because we think we can optimize the hand and wrist holder.

Plans for next quarter

The software tool is created. Once the wrist and hand holder is optimized, we will obtain good quality, full sets of images for a tendon excursion analysis. In parallel, we are developing software for the 3D geometric method for measuring tendon moment arm. Toward the end of the summer, we hope to perform both measurements on a subject. We are continuing to plan validation tests.

1.a.ii. PASSIVE AND ACTIVE MOMENTS

Abstract

During the past quarter, work has focused on modifying of an existing apparatus (Esteki and Mansour, 1996) used to measure passive moments about the finger joints. Software for passive moment data acquisition has also been written in Labview®.

Purpose

The purpose of this project is to characterize the passive properties of normal and paralyzed hands. This information will be used to determine methods of improving hand grasp and hand posture in FES systems.

Report of Progress

The passive properties of the paralyzed hand play an important role in the grasp patterns developed using electrical stimulation. The passive forces developed at a joint are due to the soft tissues surrounding the joint (ligaments, skin, joint capsule) and the tension on the tendons crossing the joint. These properties may be very different between paralyzed and normal hands. The goal of this project is to measure the passive properties of all three joints of each of the four fingers. Both normal and paralyzed properties will be measured.

In order to measure the passive moments at all the finger joints as a function of finger joint angle and finger joint velocity for different proximal joint positions, the apparatus used by Esteki (see NIH QPR#6 NO1-NS-2-2344) was modified. This device had been developed to measure the passive torque-angle properties of a single joint moved at various angular rates. The data obtained from this device have been described previously (QPR#6 NO1-NS-2-2344). The modifications were necessary to meet the following specifications:

- the device must be capable of making measurements on both right and left hands
- the configuration of the device must not interfere with the range of motion of the joint being examined
- the device must be capable of rotating each joint of each finger through its range while the other finger joints and wrist are fixed
- the adjustments of finger and wrist splints between trials must be quick and easy

As shown in Figure 1.a.ii.1., the device rotates the finger in the horizontal plane about a specific joint aligned with the apparatus' rotating shaft. The tip of the finger is attached to a vertically oriented instrumented cantilevered beam which serves as the force transducer. This beam is attached to a horizontal arm which is rotated about the shaft driven by a gear-head motor (not included in the figure). The speed of rotation is set and maintained by an electronic controller. The range of motion of each joint tested is set by mounting limit switches on a circular plate. When the horizontal arm closes either switch the motor reverses its direction of rotation. Joint angle is measured by a potentiometer mounted to the rotating shaft.

The stationary parts of the apparatus are now positioned distal to the hand rather than behind the hand, allowing the apparatus armature to sweep through 360° (without the limit switches) regardless of the position of the wrist. This means that it will be possible to measure the passive moment through the joint's entire range of motion without the device itself interfering. This improved spatial configuration also allows left hand digits to be tested as easily right hand digits. The entire apparatus has been mounted on a Delrin® sheet that fits on a high-low table, making it easier to properly position individuals in wheelchairs.

New forearm and wrist splints allow the investigator to position the subject's arm more easily and quickly at the start of a test session and between trials. An adjustable finger splint has been constructed to fix all the joints of the finger at desired positions (except the one being rotated). This will make it possible to measure passive moments at the proximal and distal interphalangeal joints as well as the at the metacarpophalangeal joint as a function of proximal and distal joint positions.

Additionally, the limit switches are now mounted with bolts rather than clips. This ensures that the switches will stay in place, keeping the finger joint from being overly flexed or extended.

A new force transducer beam mounted with four strain gages was constructed. The four strain gages allow us to measure the shear force in the beam whenever a force is exerted by the finger against the beam. Because the shear force in a beam is independent of the force's point of application along the beam, it is no longer necessary to calibrate the force transducer for each different point of force application possible along the beam. This makes data acquisition simpler.

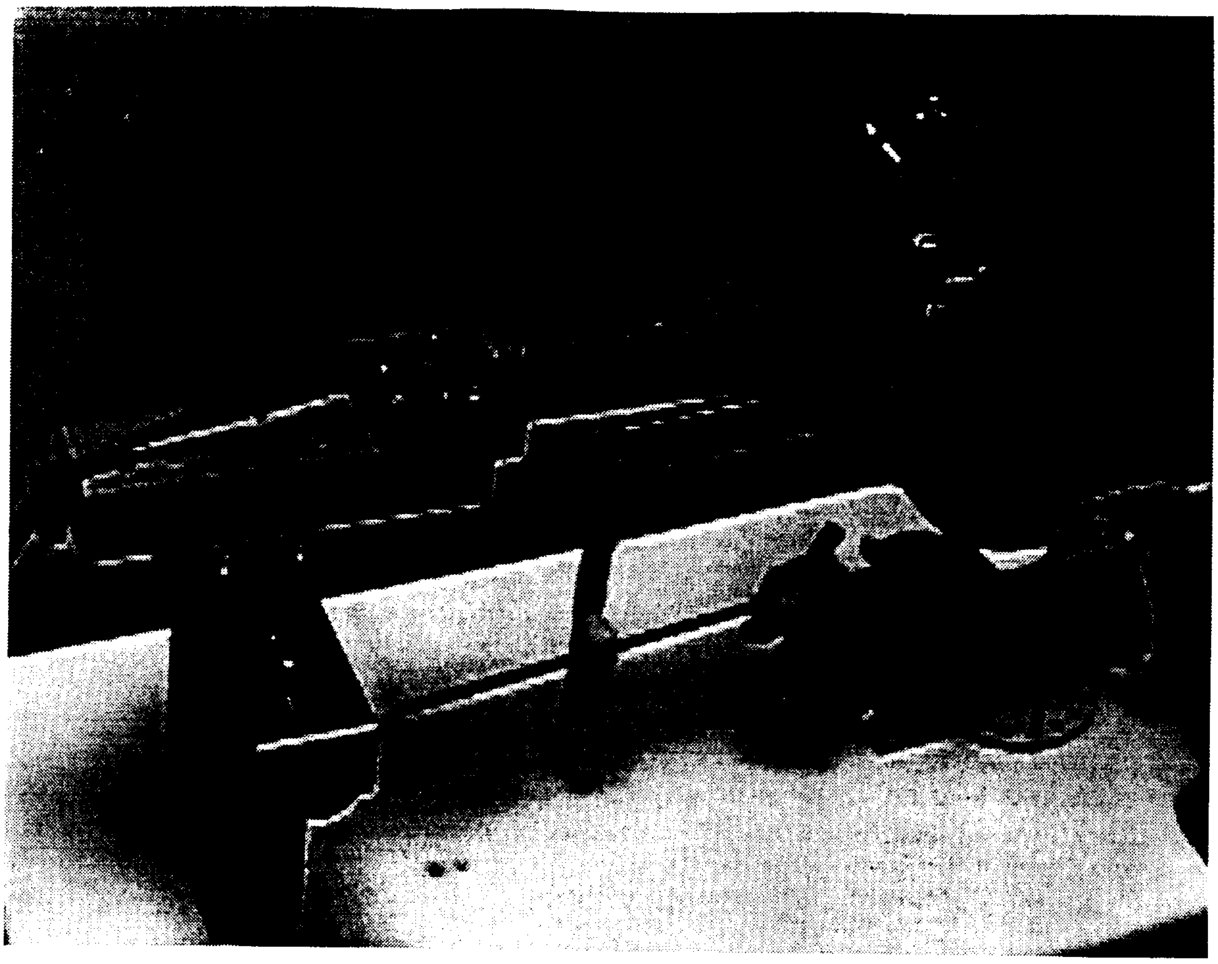

Figure 1.a.ii.a. Passive moment measuring apparatus excluding gear-head motor.

Besides the modifications made to the passive moment measuring apparatus, software for calibrating the force and angle transducers was written. Also a routine for acquiring moment-angle plots was written. In the data acquisition routine, passive joint moment, joint angle, and time are recorded simultaneously at a sampling rate of 30 Hz.

Plans for Next Quarter

The work to follow will concentrate on making preliminary measurements in order to facilitate the design of an experimental protocol. We are anticipating performing experiments with unparalyzed and paralyzed subjects this summer.

Reference

Esteki, A. and Mansour, J. M. (1996) An experimentally based nonlinear viscoelastic model of joint passive moment. *J. Biomechanics* 29, 443-450.

1. b. BIOMECHANICAL MODELING: ANALYSIS AND IMPROVEMENT OF GRASP OUTPUT

Abstract

This project does not start until year three of the project, as described in the proposal. However, two important tools are being developed in order to make the necessary biomechanical measurements with individual patients. First, the use of magnetic resonance images to determine joint moment arms is described in Section 1.a.i. Secondly, the measurement of passive moments across all joints of the hand is described in Section 1.a.ii.. When these tools are complete, we will begin making measurements on both normal and paralyzed patients.

Objective

The purpose of this project is to use the biomechanical model and the parameters measured for individual neuroprosthesis users to analyze and refine their neuroprosthetic grasp patterns.

2. CONTROL OF UPPER EXTREMITY FUNCTION

Our goal in the four projects in this section is to either assess the utility of or test the feasibility of enhancements to the control strategies and algorithms used presently in the CWRU hand neuroprosthesis. Specifically, we will: (1) determine whether a portable system providing sensory feedback and closed-loop control, albeit with awkward sensors, is viable and beneficial outside of the laboratory, (2) determine whether sensory feedback of grasp force or finger span benefits performance in the presence of natural visual cues, (of particular interest will be the ability of subjects to control their grasp output in the presence of trial-to-trial variations normally associated with grasping objects, and in the presence of longer-term variations such as fatigue), (3) demonstrate the viability and utility of improved command-control algorithms designed to take advantage of forthcoming availability of afferent, cortical or electromyographic signals, and (4) demonstrate the feasibility of bimanual neuroprostheses.

2. a. HOME EVALUATION OF CLOSED-LOOP CONTROL AND SENSORY FEEDBACK

Abstract

The purpose of this project is to deploy an existing portable hand grasp neuroprosthesis capable of providing closed-loop control and sensory feedback outside of the laboratory. Effort this quarter was

devoted to: (1) completion and submission of a manuscript describing distortions of electrocutaneous loudness and pitch present in the sensory feedback codes proposed for the portable system, (2) testing of a simple modification of the thumb-mounted force sensor that provides vastly improved performance over previous versions, (3) testing of a streamlined algorithm for calibrating the joint-angle sensors that does not require the optical motion analysis system, and (4) minor modifications of the software and compliant object for grasp-release testing.

Purpose

The purpose of this project is to deploy an existing portable hand grasp neuroprosthesis capable of providing closed-loop control and sensory feedback outside of the laboratory. The device is an augmented version of the CWRU hand neuroprosthesis, and was developed and fabricated in the previous contract period. The device utilizes joint angle and force sensors mounted on a glove to provide sensory information, and requires daily support from a field engineer to don and tune. The portable feedback system is not intended as a long term clinical device. Our goal, rather, is to evaluate whether the additional functions provided by this system benefit hand grasp outside of the laboratory, albeit with poor cosmesis and high demands for field support.

Report of Progress

Effort this quarter was devoted to: (1) completion and submission of a manuscript describing distortions of electrocutaneous loudness and pitch present in the sensory feedback codes proposed for the portable system, (2) testing of a simple modification of the thumb-mounted force sensor that provides vastly improved performance over previous versions, (3) testing of a streamlined algorithm for calibrating the joint-angle sensors that does not require the optical motion analysis system, and (4) minor modifications of the software and compliant object for grasp-release testing.

Distortion: The distortion experiments that were started in the prior contract period were completed and the results have been submitted for publication in *Perception & Psychophysics*. Measurement of isoloudness contours by Békésy tracking have been described in a previous report, and isopitch contours have been measured similarly. The results are summarized in Fig. 2.a. 1, showing the isoloudness and isopitch contours averaged across subjects. The stimulus range covered the majority of frequencies and amplitudes that will be used for sensory feedback of finger span and grasp force, respectively, in the portable system. The distortion of stimulus loudness by stimulus frequency is slight but statistically significant, and is manifest by the increased amplitudes needed at low frequencies to maintain a constant loudness. The parallel isoloudness contours also show that loudness distortion is independent of loudness level. Pitch is not distorted systematically by changing amplitudes, although the variability of the pitch matches was much higher than that of the loudness matches.

Force Sensor: The force sensor that has been described in previous reports was constructed from an Interlink force sensitive resistor (FSR) glued to a rigid substrate, with an epoxy dome built up on the force-sensitive surface of the FSR [see Jensen, T. R., R. G. Radwin, et al. (1991). "A conductive polymer sensor for measuring external finger forces." J Biomech **24**(9): 851-858]. The performance of that sensor was unacceptable. The output had significant hysteresis and was highly sensitive to the orientation of the load relative to the plane of the sensor and the location of the point of contact. We have modified the sensor assembly with remarkable results. The new assembly is shown in Figure 2. a. 2 (A), and consists of a disk of sponge rubber (approximately 2 mm thick) sandwiched between the FSR and a disk of aluminum shim stock. That assembly is then glued to a rigid substrate. In previous reports, the sensor and substrate were then sewn onto the sensor glove. However, a more efficient mounting scheme is illustrated in Figure 2. a. 2 (B). The sensor assembly is glued to a guitar thumb pick which provides both a rigid backing for the sensor and a rigid mounting surface for the sensor lead and connector. The guitar pick may then be worn with or without the rest of the sensor glove.

An example of the sensor output is illustrated in Figure 2. a. 3. The force sensor was worn on the thumb of an able-bodied subject, who pressed the sensor against a six-axis load cell. The traces in the figure show the output from the force sensor circuit versus the vertical load measured by the load cell. The different traces have been offset vertically for clarity. The bottom three traces are from three separate trials in which the thumb was pressed against the load cell several times in each trial. Note that the hysteresis is minimal. The upper three traces are from trials in which the thumb was pressed against the load cell and then intentionally "wobbled" to vary the orientation of the sensor plane relative to the vertical axis. The wobbling did not produce significant errors in the measurement of the normal force component. The thick gray lines show the stability of the sensor output across time, and represent a single logarithmic curve fit to the bottom trace and offset to coincide with the beginning of each of the other traces. Clearly, there was no significant change in the shape of the input-output characteristic across trials. The new configuration of the force sensor is superior to previous versions in all respects.

The simplicity and relative unobtrusiveness of the new force sensor suggests that it may be most appropriate to choose force feedback alone as the first condition to assess outside of the laboratory, which will obviate the need, at first, for the sensor glove. The glove can then be used in subsequent assessments.

Joint Angle Algorithm: A new algorithm for calibrating the sensor glove's joint angle sensors has been developed which greatly streamlines the procedure and does not require the motion tracking system used previously. Therefore, the procedure could be used outside of the laboratory in case the joint angle sensors need to be checked or recalibrated on site. The procedure measures the angle sensor outputs at a variety of known grasp openings determined by grasping blocks with a variety of thicknesses [as used in Van Doren, C. L. (1995). "Cross-modality matches of finger span and line length." Perception &Psychophysics **57**(4): 555-568]. The scaling coefficients for each angle sensor were then adjusted and optimized by fitting the calculated spans to the known spans via iterative nonlinear least-squares regression.

The procedure has been tested for lateral grasp using the model shown in Figure 2. a. 4 (top). The grasp opening G is given by:

$$G = L_0 \sin(\theta_0) + L_1 \sin(\theta_0 + \theta_1) + L_2 \sin(\theta_0 + \theta_1 + \theta_2)$$

where the *Ls* are measured segment lengths. The fixed radiocarpal angle (θ_0) and the gains and offsets for the joint angle sensors were adjusted iteratively to optimize the calculated grasp opening. An example of the resulting calibration is shown in Figure 2. a. 4 (bottom).

Radial and ulnar deviation of the wrist can contaminate the spans calculated from the joint angle sensors due to changes in the output of the wrist angle sensor. As a consequence, it may be necessary to add another sensor specifically to measure and compensate for radial/ulnar deviation.

Minor Modifications: A minor error was found and corrected in the assessment software for the portable system, and the compliant object used in those assessments has been modified to facilitate testing.

Plans for Next Quarter

The modifications of the portable closed-loop system will be incorporated in preparation for testing the complete assessment protocol. If the tests are successful, a neuroprosthesis user will be recruited to wear, use, and evaluate the portable system outside of the laboratory. Sensory feedback of grasp force alone may be tested first given the modest encumbrance by the thumb-mounted force sensor.

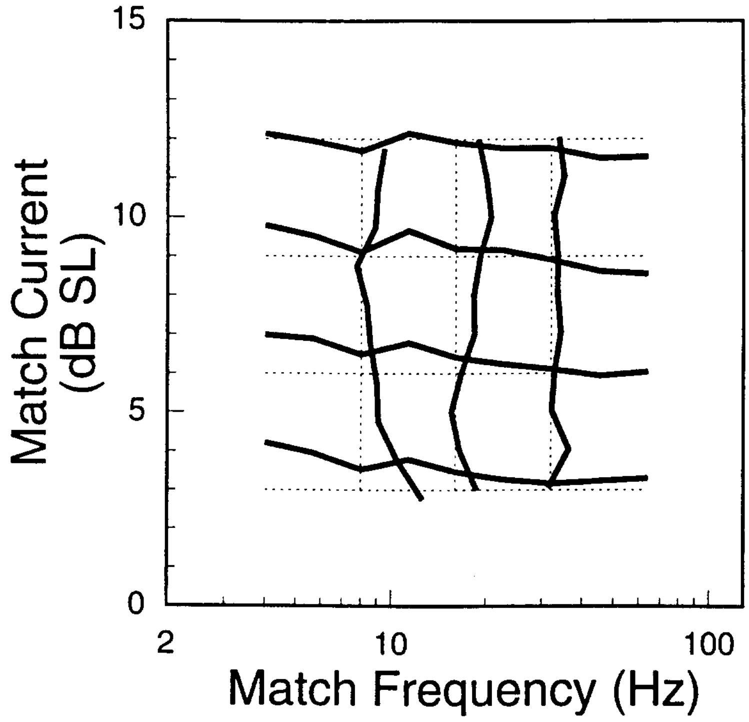

Figure 2. a. (1) Ideal and actual isopitch and isoloudness contours for electrocutaneous stimulation of the upper arm. Thin lines represent ideal, distortion-free contours. That is, perceived loudness is independent of stimulus frequency and perceived pitch is independent of amplitude. Actual contours (thick lines) are averaged across 8 subjects, with 4 repetitions per subject, and were measured using a Békésy tracking algorithm. Each isopitch contour represents the set of stimulus frequencies and amplitudes that had the same perceived pitch as a fixed reference stimulus, even though the loudnesses varied. Isoloudness contours have the complementary interpretation. Stimulus distorted perceived loudness slightly but significantly. Stimulus amplitude did not distort perceived pitch systematically, although the absence of a significant effect may be due to the higher variability inherent in pitch matching.

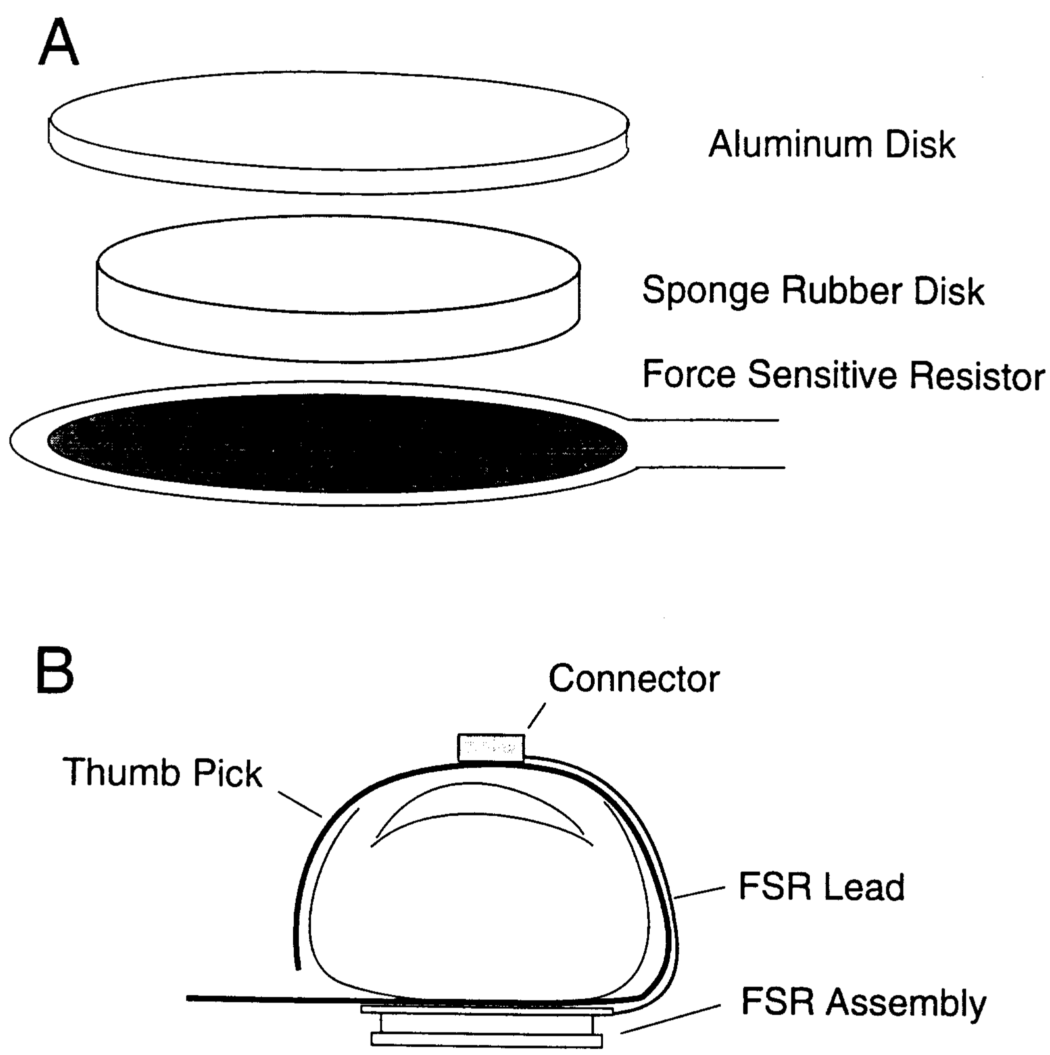

Figure 2. a. (2) Sketch of thumb-mounted force sensor construction. (A) The sensor assembly is constructed by gluing a disk of dense sponge rubber on top of the central, force-sensitive area of the FSR (Interlink, Inc.), and gluing a disk of aluminum shim stock on top of the rubber. (B) The sensor assembly is then either glued to a rigid substrate and sewn onto the sensor glove (as described in previous reports), or is glued to a guitar thumb pick which is worn on the thumb, with or without the rest of the sensor glove. The thumb pick provides both a rigid platform for the sensor and a rigid substrate for the FSR lead and connector.

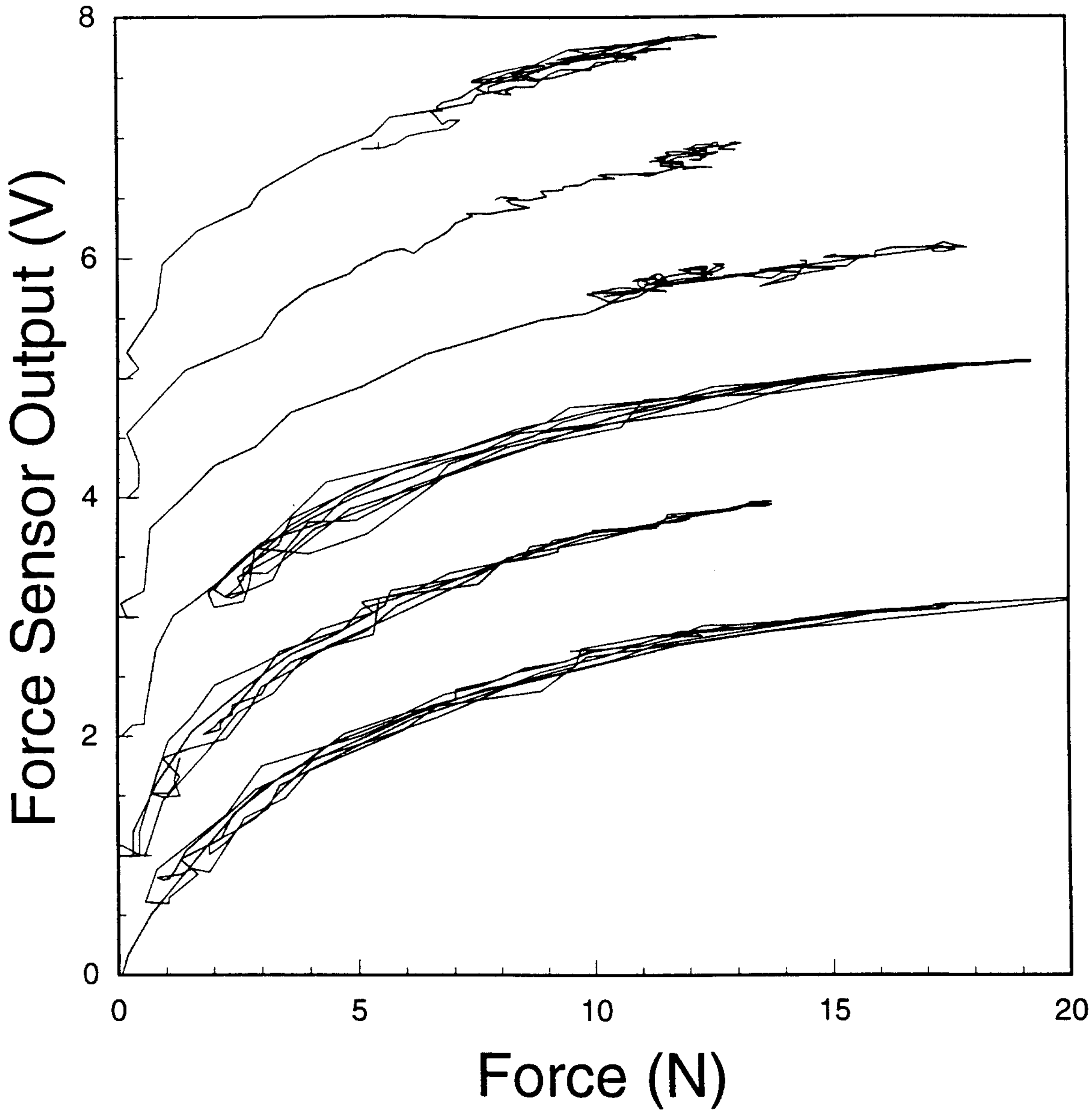

Figure 2. a. 3 Plots of thumb-mounted force sensor output versus normal contact force. The normal force was measured using a 6-axis load cell. The thumb sensor consisted of a force sensitive resistor configured as shown in the previous figure. Different traces are offset vertically for clarity. The bottom three traces show trials with the sensor worn on a subject's thumb and pressed normal to the surface of the load cell. Each trial consisted of multiple sequential presses to examine hysteresis. The upper three traces show trials in which the sensor was pressed against the load cell and then "wobbled" voluntarily to examine the effects of off-axis forces. The thick gray lines represent a logarithmic fit to the lowest trace which was then duplicated and offset to demonstrate the stability of the sensor's output across trials.

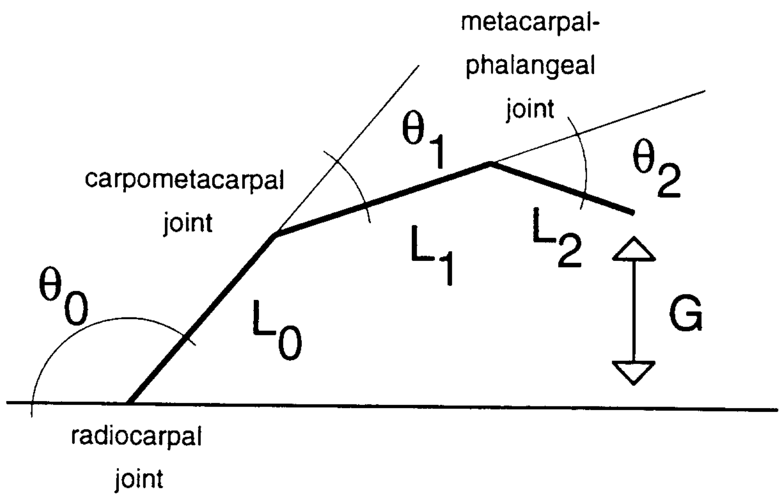

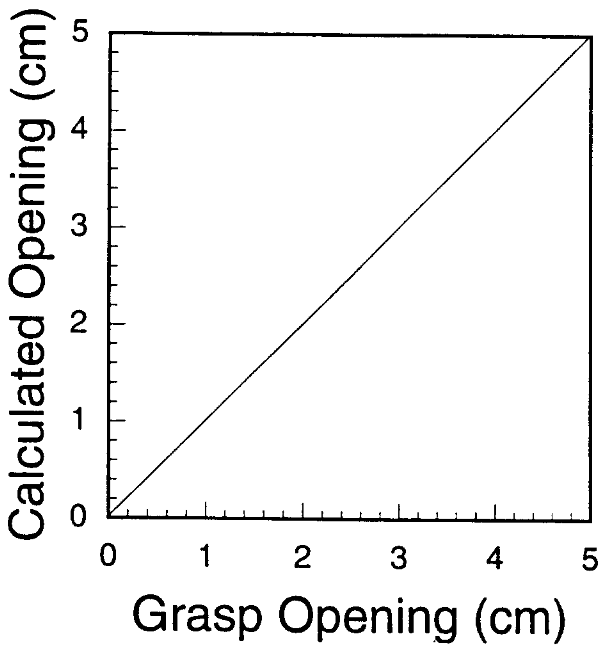

Figure 2. a. 4. Joint angle sensor calibration. (Top) Sketch of thumb model for calculating grasp opening *G* from output of joint angle sensors at CMC and MP joints. The IP joint is assumed fixed. The segment lengths *L* are measured. The radiocarpal angle and the gains and offsets for the two joint angle sensors are adjusted iteratively to optimize the fit between the actual and calculated grasp opening. (Bottom) Plot of fitted versus actual grasp opening for multiple pinches of a standard set of wood blocks.

2. b. INNOVATIVE METHODS OF CONTROL AND SENSORY FEEDBACK

2. b. i. ASSESSMENT OF SENSORY FEEDBACK IN THE PRESENCE OF VISION

Abstract

The purpose of this project is to develop a method for including realistic visual information while presenting other feedback information simultaneously, and to assess the impact of feedback on grasp performance in the presence of such visual information. A new student has been recruited to perform the project, and some technical work has been completed in selection of the video simulation system components and programming of PCI-based data acquisition software.

Purpose

The purpose of this project is to develop a method for including realistic visual information while presenting other feedback information simultaneously, and to assess the impact of feedback on grasp performance. Vision may supply enough sensory information to obviate the need for supplemental proprioceptive information via electrocutaneous stimulation. Therefore, it is essential to quantify the relative contributions of both sources of information.

Report of Progress

Progress this quarter has been limited since the graduate student originally slated to conduct the research chose to pursue a different project. A new student has been recruited, however, and will be assuming responsibility for the project in mid July.

The original specifications and components chosen for the video simulation system have been reviewed. New information indicates that the video board (VideoSpigot) originally chosen will not work in this application, and other boards have been researched. The VideoVision Studio II board is the most likely candidate (alternatives are the Targa 2000 or Media 100QX boards), and will allow the use of real time hardware JPEG compression instead of storing uncompressed video clips in RAM. The increased cost of the VideoVision Studio II board will be offset in part by reduced RAM requirements. A computer and fast and wide drive still need to be chosen. A Macintosh 7500 or 8500 appears to be the best choice for video-intensive applications.

The use of either PowerPC computer will require transporting software to the new PCI-bus architecture. Several crucial components of the software, particularly those that access computer hardware (e.g., timers), have been rewritten to accommodate the change in platform. The interrupt drivers used with the data acquisition cards must still be rewritten.

Plans for Next Quarter

The software revisions for the PowerPC will be completed. The new student will begin working on the project and will finish specifying and ordering the components. If delivery is timely, the components will be assembled and new software for acquiring and displaying the video will be written.

C. 2. b. ii. INNOVATIVE METHODS OF COMMAND CONTROL

Abstract

During this quarter we developed hardware and software to measure and evaluate the signals generated by nail mounted strain gages for object contact detection during grasp.

Purpose

The purpose of this project is to improve the function of the upper extremity hand grasp neuroprosthesis by improving user command control. Command control has not been investigated as aggressively as closed-loop control and sensory feedback, but it is no less important. It is particularly appropriate to revisit the issue in the new project since we are specifically interested in designing algorithms that can take advantage of promising developments in (and forthcoming availability of) alternative command signal sources such as EMG, and afferent and cortical recordings. The specific objectives are to identify and evaluate alternative sources of logical command control signals, to develop new hand grasp command control algorithms, to evaluate the performance of new command control sources and algorithms with a computer-based video simulator, and to evaluate neuroprosthesis user performance with most promising hand grasp controllers and command control sources.

The first objective is to identify and evaluate alternative sources of logical command control signals. We will investigate object contact and object slip detection using sensors mounted on the dorsal surface of the thumb. The first sensor to be investigated is a strain gage glued to the thumbnail and used to detect object contact.

Report of Progress

During this quarter we developed hardware and software to evaluate contact sensor outputs during grasp. A strain gage amplifier incorporating bridge excitation voltage, amplification, and low pass filtering was designed and fabricated. The circuit was built around an Analog Devices 1B31 bridge amplifier chip, and for this application the excitation voltage was set at 5V, the gain was left adjustable via a 10-turn precision potentiometer, and the cut-off frequency of the low pass filter was selectable with a 4-position switch from 20Hz, 50Hz, 100Hz, and 200Hz. This amplifier will be used to condition signals from strain gages mounted on a fingernail during grasp and release.

A software program for data sampling and experimental control was written using LABView software (National Instruments, Austin, TX). The program includes a virtual chart recorder to sample the output of nail mounted strain gages during grasp and release of objects. The software included a provision to provide timing cues to the experimental subject. These cues prompted the subject to acquire, lift, and replace the object within intervals set by the experimenter. However, the overhead associated with LABView did not allow accurate timing of these software prompts. Currently two alternatives methods of providing timing prompts to the experimental subjects are being investigated. First, hardware timing signals generated using counter/timers present on the National Instruments Multifunction I/O Board should eliminate the overhead associated with the LABView Software. These timers, however, can be programmed from LABView, thus preserving the integrated experimental environment. The TTL outputs from the counter/timers will be coupled to a set of LEDs to provide cues to the experimental subject. The second alternative is to use a software module written in C that can be interfaced within the LABView environment.

Plans for Next Quarter

During the next quarter we will complete development of software for experimental control and rectify the timing problem. We will then use the hardware and software developed to measure the output of nail mounted strain gages during grasp. We will conduct experiments on 5 able-bodied individuals, with each subject completing 90 trials. Six different objects will be used and 15 trials will be performed with each object.

2. b. iii. INCREASING WORKSPACE AND REPERTOIRE WITH BIMANUAL HAND GRASP

Purpose

The purpose of this project is to extend the functional capabilities of the person who has sustained spinal cord injury and has tetraplegia at the C6 level by providing the ability to grasp and release with both hands. As an important functional complement, we will also provide improved finger extension in one or both hands by implantation and stimulation of the intrinsic finger muscles. Bimanual grasp is expected to provide these individuals with the ability to perform over a greater working volume, to perform more tasks more efficiently than they can with a single neuroprosthesis, and to perform tasks they cannot do at all unimanually.

Report of progress

Effort was devoted to developing instrumentation this quarter. A more detailed report of progress will be postponed until next quarter.

2. b. iv CONTROL OF HAND AND WRIST

Abstract

Wrist extension moments must be capable of balancing the flexion moments in order to establish an equilibrium in a functional position. Extension moments can be generated by residual voluntary extension, by voluntary extension of a transferred brachioradialis, or by stimulation of a transferred extensor carpi radialis. We have found that the combination of a transferred and stimulated extensor carpi radialis, combined with voluntary extension is necessary in some people, rather than relying on one mechanism alone.

Purpose

The goal of this project is to design control systems to restore independent voluntary control of wrist position and grasp force in C5 and weak C6 tetraplegic individuals. The proposed method of wrist command control is a model of how control might be achieved at other joints in the upper extremity as well. A weak but voluntarily controlled muscle (a wrist extensor in this case) will provide a command signal to control a stimulated paralyzed synergist, thus effectively amplifying the joint torque generated by the voluntarily controlled muscle. We will design control systems to compensate for interactions between wrist and hand control. These are important control issues for restoring proximal function, where there are interactions between stimulated and voluntarily controlled muscles, and multiple joints must be controlled with multijoint muscles.

Report of progress

Our report this quarter will summarize the results of experiments to date that examine the balance of moments at the wrist.

Stimulation of the extrinsic flexor hand muscle generates large flexion moments at the wrist. Thus in order to provide wrist stability, an extension moment at the wrist must be generated. Extension moments at the wrist can be produced by the following methods: (1) voluntary effort (by residual voluntarily controlled ECRL / ECRB, or by voluntary tendon transfer of BRD to ECRB), (2) stimulation of ECU transferred to ECRB, or (3) combination of (1) and (2). To hold the wrist in extension during grasp, the extension moment generated at the wrist by either (1), (2), or (3) must be greater than the flexion moment generated at the wrist by the neuroprosthesis. The net wrist moment was measured during grasp activation plus voluntary effort and/or ECU stimulation to determine which method of wrist extension resulted in a net wrist extension moment during grasp activation.

Methods

Measuring Apparatus The subject's arm was strapped in an open cast mounted on a table in order to prevent movement proximal to the wrist. The palm of the hand was strapped to a splint that was attached to a universal joint with a steel rod. The forces exerted at the universal joint by the wrist were measured with a six axis force moment transducer (JR^3, Inc.). The wrist moment was found by multiplying the moment arm (distance from the universal joint to the capitate head of wrist) by the force measured by the transducer.

Experimental Conditions The net wrist moment was measured under six conditions: (1) maximum voluntary wrist extension, (2) stimulation of ECU transferred to ECRB, (3) palmar and lateral grasp activation, (4) maximum voluntary wrist extension with grasp activation, (5) ECU stimulation with grasp activation, and (6) grasp activation with ECU stimulation combined with maximum voluntary wrist extension. During these measurements, the wrist was held at either 20° extension or 45° extension.

Subjects The measurements described in the previous section were conducted on five subjects. Four out of the five subjects had voluntary wrist extension, either weak residual or by voluntary tendon transfer of BRD -> ECRB. Subject #4 did not have voluntary wrist extension (Table 2. b. iv.1). All five subjects had undergone the ECU -> ECRB transfer. During the experiments, the neuroprosthesis was controlled by the experimenter rather than the subject. Some subjects were studied at the Baltimore VA Medical Center as part of a collaboration with Dr. Peter Gorman.

Subject	Voluntary Wrist Extension
#1	weak residual
#2	BRD->ECRB
#3	BRD -> ECRB
#4	none
#5	BRD->ECRB

Table 2. b. iv.1 Subjects Participating in Wrist Moment Experiments

Results

I. Transferring ECU -> ECRB can Provide Strong Wrist Extension Moment

The ECU is innervated in C5/C6 population; however, it is primarily an ulnar deviator. The ECRB is a strong wrist extensor, but it is dennervated in this population. Therefore, by transferring the ECU to the ECRB, a stronger wrist extension moment should be generated. The wrist moment generated by stimulating the ECU before and after transfer to the ECRB was recorded in two subjects and is shown in Figure 2. b. iv.1. For both subjects, the stimulated transferred ECU produced a stronger wrist extension moment.

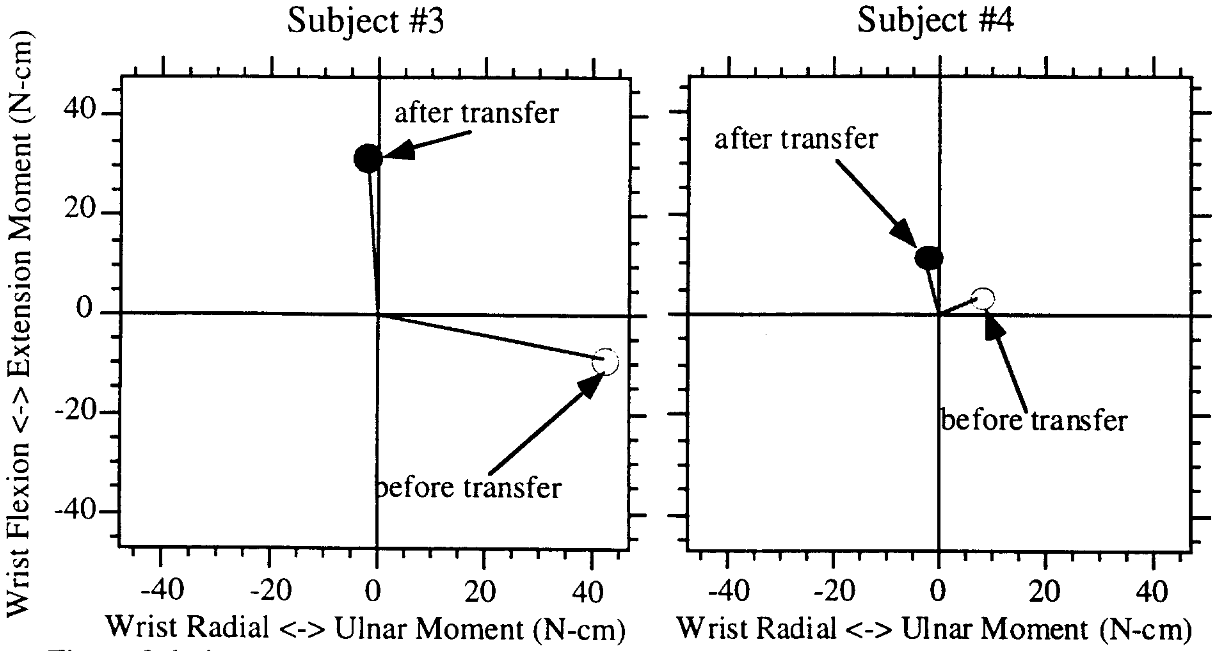

Figure 2. b. iv.1 Wrist Moment Generated by Stimulating ECU Before and After Transfer to ECRB

II. Counterbalance of Grasp Flexion Moment at Wrist by Voluntary Wrist Extension and/or Stimulation of Transferred ECU

The individual moments produced by voluntary extension, grasp activation, stimulation of the transferred ECU, and passive forces were measured for each subject. Then, the net wrist moment was measured during grasp activation combined with either voluntary wrist extension, stimulated ECU transfer, or both to determine which combination was able to produce a net wrist extension moment. Figures 2. b. iv.2, 2. b. iv.3, and 2. b. iv.4 show the individual and net wrist moments during palmar grasp for three subjects (wrist held at 20° extension).

Individual Contributions to Wrist Moments Figure 2. b. iv.2 shows the individual moments that contribute to the net wrist moment for three subjects. All three subjects were able to produce a voluntary wrist extension moment. Also, palmar grasp generated a large, primarily wrist flexion moment (25 N-cm to 37 N-cm). However, the strength of the stimulated ECU transfer differed per subject, with the stimulated ECU of Subject #1 generating the largest wrist extension moment, and the ECU of Subject #2 generating the smallest wrist extension moment.

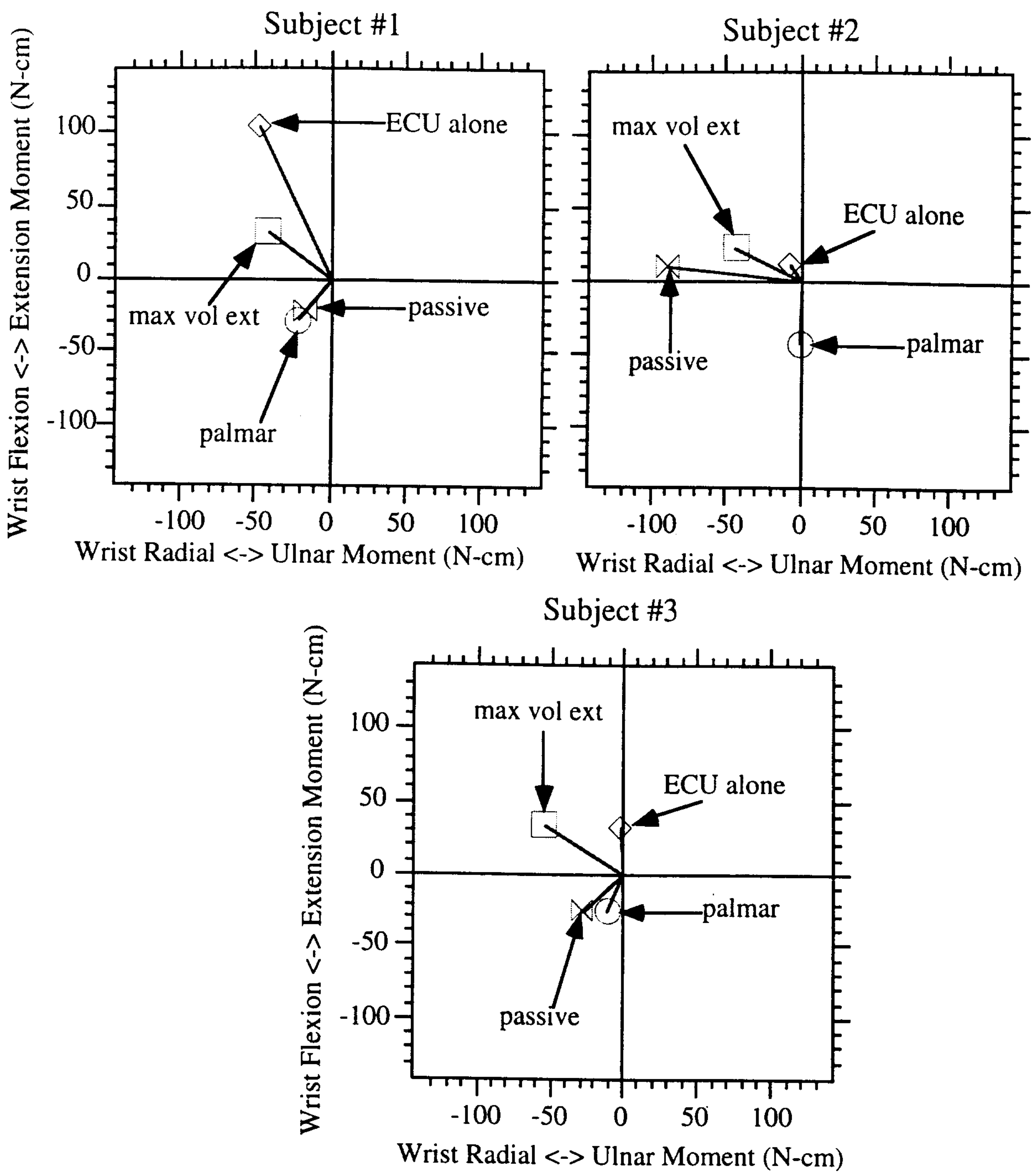

Figure2. b. iv. 2 Individual Contributions to Wrist Moment

Individual Muscles Combined with Grasp Activation Figure 2. b. iv.3 shows the net wrist moment generated during palmar grasp combined with either voluntary wrist extension or stimulated ECU transfer. For all three subjects, voluntary extension was insufficient in overcoming wrist flexion during grasp. Furthermore, the moment generated by ECU stimulation was strong enough to produce a net wrist extension moment for only one subject (Subject #1, where ECU stimulation generated the largest extension moment compared to the other subjects-see Figure 2. b. iv.2). Thus, individual muscles were not strong enough to overcome wrist flexion during grasp.

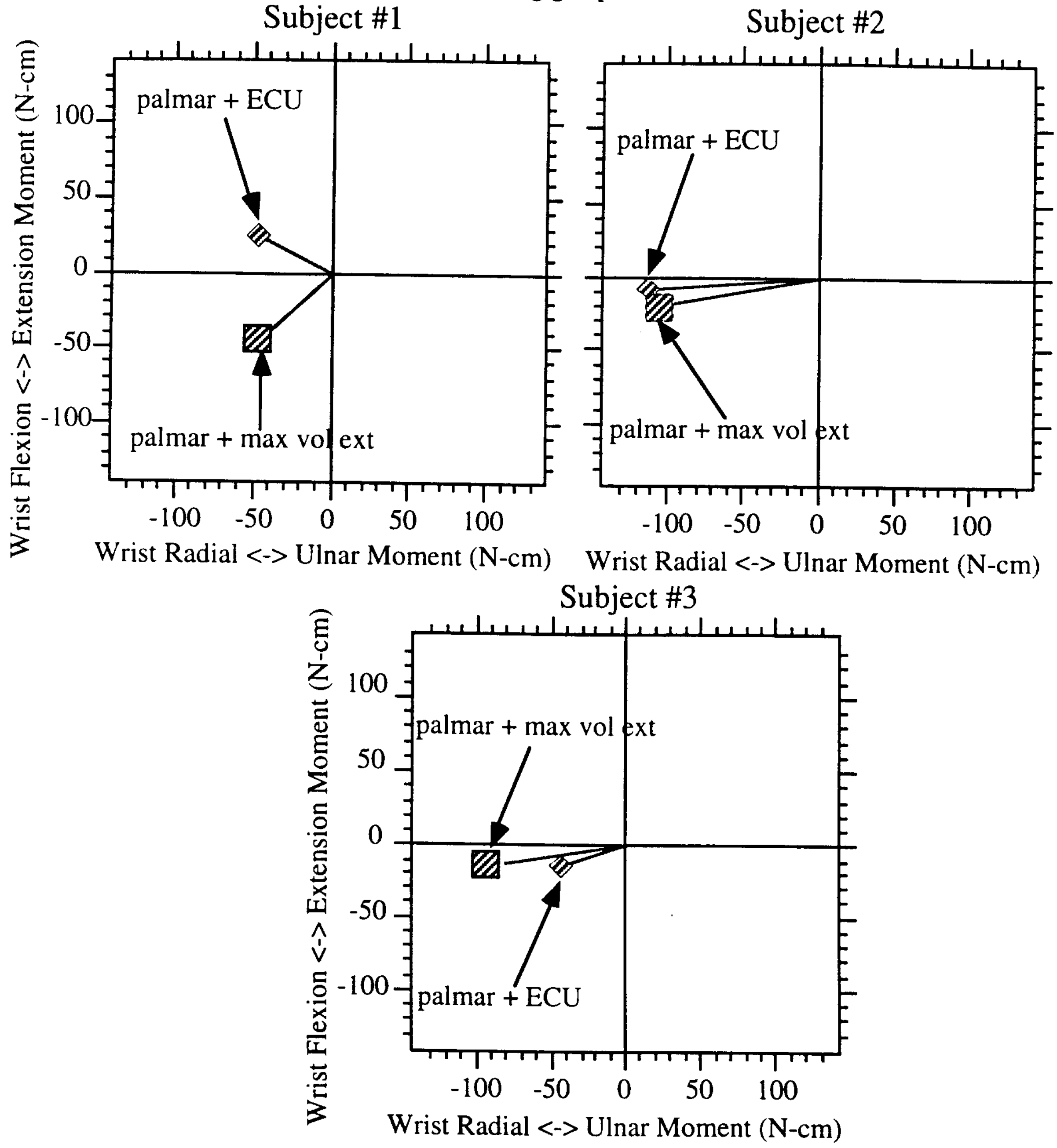

Figure 2. b. iv.3 Net Wrist Moment during Palmar Grasp with Maximum Voluntary Effort or Stimulated ECU Transfer

Combination of Voluntary Extension and Stimulated ECU Transfer during Grasp Activation
Figure 2. b. iv.4 shows the net wrist moment generated during palmar grasp combined with voluntary extension and stimulated ECU transfer. For all three subjects, the combination of ECU stimulation and voluntary effort resulted in a net wrist extension moment.

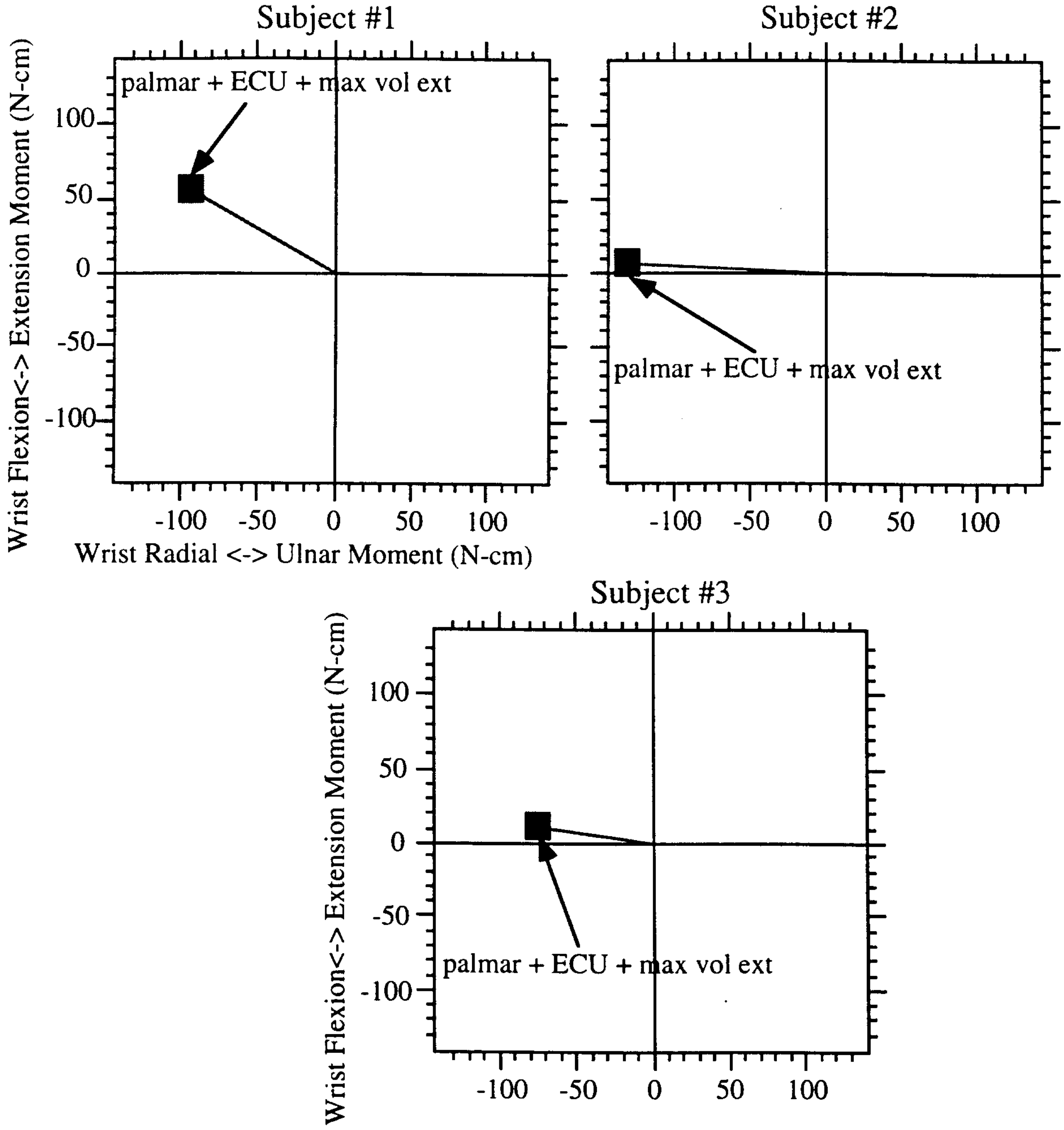

Figure 2. b. iv.4. Net Wrist Moment during Palmar Grasp with Maximum Voluntary Effort and Stimulated ECU Transfer

Summary of Wrist Moment Experiments Table 2. b. iv.2 provides a summary of whether voluntary effort, stimulation of transferred ECU, or both were sufficient in overcoming wrist flexion during grasp for all five subjects (results are the same regardless of grasp mode). All subjects except #4 had voluntary wrist extension (either by weak residual or by BRD -> ECRB transfer). Although voluntary wrist extension reduced the flexion moment generated during grasp activation, it was not strong enough to produce a net wrist extension moment. Furthermore, the wrist extension moment generated by the transfer of ECU to ECRB was strong enough to produce a net wrist extension moment during grasp for only two subjects. However, the combination of voluntary effort and stimulated transferred ECU was able to provide a wrist extension moment for all the subjects.

Subject	Vol. Wrist Ext?	Vol. Wrist Ext. counteract H.G. Flexion?	ECU->ECRB counteract H.G Flexion?	Vol. Wrist Ext + ECU->ECRB counteract H.G. Flexion?
#1	weak residual	no	yes	yes
#2	BRD -> ECRB	no	no	marginal
#3	BRD -> ECRB	marginal	marginal	yes
#4	no	not applicable	marginal	not applicable
#5	BRD -> ECRB	no	yes	yes

Table 2. b. iv.2 Summary Table for Wrist Moment Experiments